

## Biological Properties of Itraconazole-SLN

Virginia Fuochi<sup>1</sup>, Claudia Carbone<sup>2</sup>, Giulio Petronio Petronio<sup>1</sup>, Roberto Avola<sup>1</sup>, Daniele Tibullo<sup>1</sup>, Cesarina Giallongo<sup>1</sup>, Fabrizio Puglisi<sup>3</sup>, Ildebrando Patamia<sup>1</sup>, Rosario Pignatello<sup>2</sup>, Pio Maria Furneri<sup>1,\*</sup>

<sup>1</sup>Università degli Studi di Catania, Dipartimento BIOMETEC, via Santa Sofia 97, 95123 Catania, Italy

<sup>2</sup>Università degli Studi di Catania, Dipartimento di Scienze del Farmaco, Laboratory of Drug Delivery Technology, Città Universitaria, 95125 Catania, Italy

<sup>3</sup>Università degli Studi di Catania, Dipartimento di Specialità Mediche e Chirurgiche, sez. di Ematologia, via Santa Sofia 84, 95123, Catania, Italy

\*corresponding author e-mail address: [furneri@unict.it](mailto:furneri@unict.it)

## ABSTRACT

Itraconazole (ITZ) belongs to azoles, an important family of antifungal drugs, and has been used for more than 30 years in clinical applications. These drugs inhibit lanosterol 14-demethylase, the enzyme that converts lanosterol to ergosterol. As recently demonstrated, topical formulations of ITZ in solid lipid nanoparticles (SLN) and a coating layer of didodecyldimethylammonium bromide (DDAB) induce a decrease in cell viability for tumor cell lines SK-MEL-5 and A431. This potentiality of repurposing ITZ activity by using the combined nanoencapsulation strategy with the positively charged coating of DDAB prompted us to investigate such a feature versus other tumor cell lines, like malignant blood cells. The purpose of this *in vitro* study was to evaluate the antimycotic activity of neutral and cationic solid lipid nanoparticles (SLN and c-SLN, respectively), both unloaded and loaded with ITZ. Moreover, the cell viability after 24 h exposure of the histiocytic lymphoma cell line U937 was also investigated, with or without the addition of alpha-lipoic acid (ALA). Results highlighted the activity of ITZ-SLN; in particular, both neutral and cationic unloaded SLN, as well as neutral drug-loaded SLN, were found to be inactive. Improvements of the MIC<sub>50</sub> value against *Candida albicans* strains were found for neutral ITZ-SLN (MIC<sub>50</sub> was 0.006 µg/ml) and cationic ITZ-SLN (MIC<sub>50</sub> equal to 0.004 µg/ml) (the MIC<sub>50</sub> value for free ITZ was 0.015 µg/ml). Moreover, the SLN induced an anti-proliferative effect on lymphoma cells at 1 µg/ml. ALA did not modify the cellular proliferation of cells but its combination with the SLN showed, even with a certain improvement, that it was not able to recover the cellular vitality.

**Keywords:** Itraconazole (ITZ), Solid Lipid Nanoparticles (SLN), cationic SLN, didodecyldimethylammonium bromide (DDAB), alpha-lipoic acid (ALA), U937 cell line.

## 1. INTRODUCTION

In recent years, more and more attention has been paid to drug delivery systems that could improve the pharmacokinetic and drug dynamics properties.

Compared to other delivery systems, Solid Lipid Nanoparticles (SLN) play an increasingly predominant role, since these formulations can merge a controlled drug release and a chemical stabilization of the loaded molecules, with a greater physical stability and shelf-life of the whole formulation [1-3]. The effectiveness of these new formulations loaded with antibacterial compound (such as ciprofloxacin and erythromycin) has been recently documented by our research group [4, 5]. Despite this, their use with antifungal drugs is not yet fully investigated [6, 7]. Among the various classes of available antimycotics, azole derivatives play a predominant role in the treatment of fungal infections. Triazoles are considered the drugs of choice in the treatment of invasive and allergic fungal infections. They act by inhibiting an enzyme of ergosterol synthesis (14- $\alpha$ -demethylase).

Itraconazole (ITZ) was the first triazole available orally, but its high lipophilicity makes it poorly soluble at physiological pH and almost totally linked to plasma proteins [8]; these features make it an excellent candidate for the formulation with SLN. Moreover, what makes this molecule even more valuable in clinical practice is its potential anticancer activity [9-12].

In particular, topical SLN formulations loaded with ITZ and having a positively-charged coating layer of didodecyldimethylammonium bromide (DDAB) induced a decrease in cell viability of the tumour cell lines SK-MEL-5 and A431 [7].

The purpose of this *in vitro* study was to investigate the antimycotic activity of cationic (cSLN) and neutral SLN, both unloaded and loaded with ITZ. Moreover, the cytotoxicity of ITZ-cSLN, with or without the addition of alpha-lipoic acid (ALA), against histiocytic lymphoma cell line U937 was also studied.

## 2. EXPERIMENTAL SECTION

**Materials.** Suppocire NB (C<sub>10</sub> - C<sub>18</sub> triglycerides) was provided by Gattefossè (Milan, Italy). Tegin O (glyceryl monooleate) and Brij 98 (Oleth-20) were purchased from ACEF (Piacenza, Italy). Didecyldimethylammonium bromide (DDAB), Tween<sup>®</sup> 80 (polysorbate 80), [3-(4,5-dimethylthiazol-2-yl)-2,5-diphenyltetrazolium bromide] (MTT) and itraconazole (ITZ) were

purchased from Sigma-Aldrich srl (Milan, Italy). All HPLC solvents (LC grade) were from Merck KGaA (Darmstadt, Germany).

**Nanoparticle production.** The SLN were prepared as previously described [7]. An oily phase, consisting of 9% w/w of Suppocire NB and 13.3% w/w of the surfactants mixture (Oleth-20/Tegin O,

2:1 weight ratio) was heated to ~80°C. Water, warmed at the same temperature, was added dropwise and under stirring to the oily phase, while keeping the temperature constant; the mixture was thereafter cooled to 60°C. The formulation was exposed to three thermal cycling of heating and cooling (80–60°C) and finally cooled in an ice bath for 2 h, under constant agitation. DDAB (0.15% w/w) and/or ITZ (0.05% w/w) were added to the oily phase to prepare, respectively, positively charged nanoparticles (cSLN) and drug-loaded formulations (ITZ-SLN and ITZ-cSLN).

**Physicochemical characterization.** Mean particles size (Zave), polydispersity (PDI) and Zeta potential (ZP) values of the produced SLN were determined by photon correlation spectroscopy (PCS) using a Zetasizer Nano S90 (Malvern Instruments, Malvern, UK). Each analysis was performed in triplicate after diluting the sample (50 µL) in ultra purified water (1 ml).

**Turbiscan® AG Station.** Stability studies were performed on the native concentrated colloidal dispersions at three different storage temperatures (25, 40 or 60°C) using the optical analyzer Turbiscan® Ageing Station (TAGS, Formulation, L'Union, France). Ten ml of each SLN suspension were placed in a cylindrical glass cell and stored in the Turbiscan for 30 days. The detection head, composed of a pulsed near-infrared light source ( $\lambda = 880$  nm) and two synchronous transmission (T) and backscattering (BS) detectors, scanned the entire height of the sample cell (65 mm longitude), at every 40 µm (1625 acquisitions for each scan), acquiring the value of T at 180° from the incident beam.

**Encapsulation efficiency and *in vitro* drug release.** ITZ encapsulation efficiency (EE%) was determined by ultracentrifugation of the SLN suspensions; the pellet was dispersed in acetonitrile, vortexed and analyzed by HPLC. The encapsulation efficiency was calculated as reported in Eq. 1, by the ratio between the amount of drug encapsulated in the nanoparticles and the amount of drug weighted for the preparation:

$$\text{(Eq. 1) } EE\% = \frac{\text{(amount of drug entrapped)}}{\text{(total amount of drug used)}} \times 100$$

ITZ release was evaluated by dialysis, placing 1 ml of SLN in a regenerated cellulose membrane dialysis bag (Spectra/Por CE; MWCO: 3000) (Spectrum, Los Angeles, CA, USA) sealed at both ends. Each bag was placed into a beaker containing 30 ml of saline

(0.9%, NaCl w/v), under controlled temperature ( $37 \pm 0.1^\circ\text{C}$ ) and constant stirring (350 rpm) for 24 h. At fixed time intervals, aliquots of the receptor phase were withdrawn and replaced with the same volume of fresh saline, and analyzed by HPLC, using a Varian Prostar model 230 (Varian, Milan, Italy), equipped with an auto-sampler Varian Model 410 and Galaxie software. To determine the percentage of drug released, a reversed-phase C18 column (Lichrospher 100 RP-18, 5 microns, 4×250 mm) (VWR, Milan, Italy) was used. A mixture of water/acetonitrile (30:70 v/v) at a flow rate of 0.8 ml/min was used as the mobile phase. Samples were analyzed at a  $\lambda$  value of 262 nm.

**Statistical analysis.** Statistical analysis was performed by Student's *t*-test ( $p < 0.05$ ) using the Origin Software package (version 8.5.1).

**Cell cultures.** U937 cell line (histiocytic lymphoma cells) was obtained from American Type Culture Collection (Merck KGaA, Darmstadt, Germany). Cell lines were maintained in RPMI medium containing 2 mM L-glutamine, 10% v/v fetal bovine serum (FBS), 100 U/ml penicillin and 100 µg/ml streptomycin, at 37°C in a humidified incubator providing 5% CO<sub>2</sub>.

**Cell viability assay.** Cells were seeded in 96-well plates at  $1 \times 10^3$  cells/well. After 24 h of treatment with the four SLN suspensions (loaded or not loaded, and neutral or cationic), 20 µL of MTT solution (5 mg/ml) were added to each well. Then, after 3 h of incubation, formazan crystals were dissolved in 150 µL of 0.1 M HCl in isopropanol. Colour intensity was measured at 570 nm with an ELISA plate reader (Thermo Scientific Multiskan FC, Waltham, MA, USA).

**Antifungal Assay.** The growth inhibitory activity against 25 *Candida* strains was determined following the Clinical and Laboratory Standards Institute document M27-A3, as previously described [13, 14]. Briefly, a suspension of an overnight culture of each strain of *Candida* was prepared in sterile saline (0.85% NaCl, w/v) and adjusted to  $1.0 \times 10^6$  CFU/ml. Then, another dilution was made to obtain a concentration of  $1.0 \times 10^4$  CFU/ml in RPMI 1640 medium. 100 µL of *C. albicans* suspensions in RPMI broth and 100 µL of fresh RPMI were added to each well of a sterile 96-well microplate (Thermo Scientific Sterilin™, Waltham, MA, USA). Plates were incubated aerobically at 35°C for 24–48 h, and minimum inhibitory concentration values (MICs) were recorded at 490 nm (OD) using a microplate reader (Gen5 Microplate Reader, BioTek Instruments, Winooski, VT, USA).

### 3. RESULTS SECTION

The phase inversion temperature (PIT) method, a low-energy method reported in the literature for the production of lipid nanoparticulate systems [15, 16], allowed us to produce a clear colloidal suspension characterized by the typical bluish-colored shade, suggesting the presence of small homogeneously dispersed nanoparticles. PCS results confirmed the presence of small particles of about 30 nm with high size homogeneity (PDI = 0.185). The addition of the positively charged layer of DDAB on nanoparticle surface induced an increase of mean particles size, which however remained below 100 nm (Table 1).

**Table 1.** Mean particles size (Zave), polydispersity (PDI), zeta potential (ZP) and encapsulation efficiency (EE%) of unloaded SLN and coated with DDAB cSLN, analysed after their preparation. Data represent the mean of at least three experiments  $\pm$  standard deviation (SD).

Sample	Zave (nm) $\pm$ S.D.	PDI $\pm$ S.D.	ZP (mV) $\pm$ S.D.
SLN	25.98 $\pm$ 1.89	0.155 $\pm$ 0.006	-10.06 $\pm$ 0.05
cSLN	60.50 $\pm$ 0.51	0.260 $\pm$ 0.005	28.6 $\pm$ 1.12

The addition of DDAB turned the ZP values from negative to extremely high positive values, increasing the stability of the SLN

formulation in respect to the uncoated colloidal suspension, in agreement with previous findings [17-21]. In particular, stability studies performed by Turbiscan technology showed both tested formulations had a great physical stability, since no significant variation of  $\Delta T$  was observed (values < 20%), thus confirming the absence of relevant instability phenomena in terms of particles migration and/or aggregation (Figure 1a).

ITZ (having a logP around 5.7) was successfully encapsulated in both uncoated and positively charged SLN, with EE% values of 76 and 98, respectively, thus confirming the ability of SLN in loading high amount of poorly water-soluble drugs [22]. Furthermore, drug incorporation did not modify the mean particle size and PDI in respect to unloaded SLN (data not shown), suggesting its ordinate allocation within the lipid matrix of the system. According to literature findings, SLN provided a sustained and prolonged drug release, without any relevant burst effect, with a quicker and higher release of the drug from positively charged SLN (Figure 1b), due to the presence of the cationic lipid on the SLN surface and the resulting lipid-water interface [7, 18, 19, 23].

Antifungal activity of free and nanoencapsulated ITZ, defined as the MIC value, i.e., the prominent decrease in turbidity corresponding to approximately 50% inhibition of growth was determined spectrophotometrically. The results are reported in Table 2.

**Table 2.** *In vitro* antimycotic activity of unloaded and ITZ-loaded neutral and cationic SLN evaluated at 24 and 48 h against 25 strains of *Candida albicans*.

Sample	(µg/ml) 24 h		(µg/ml) 48 h	
	MIC <sub>50</sub>	MIC <sub>90</sub>	MIC <sub>50</sub>	MIC <sub>90</sub>
ITZ	0.015	0.03	0.015	0.03
SLN	No inhibition	No inhibition	No inhibition	No inhibition
cSLN	No inhibition	No inhibition	No inhibition	No inhibition
ITZ-SLN	0.006	0.006	0.006	0.006
ITZ-cSLN	0.004	0.007	0.007	0.007

Once loaded in the SLN, and in particular, in loaded DDAB-coated cSLN, ITZ showed a reduction of MIC values, in the order of one to three dilutions compared to free drug, for all the tested *Candida* strains. Noteworthy, the gain in terms of MIC reduction remained stable even at 48 h.

Although it has been previously noted that unloaded SLN coated with DDAB showed some inhibitory activity against bacteria [4], most probably due to the effects of the cationic lipid upon the bacterial cell membrane, such a feature was not evidenced with *Candida albicans* in our experimental conditions.

Treatment of histiocytic lymphoma cell line U937 with the same specimens (Figure 2) showed an anti-proliferative effect at the concentrations tested (1 µg/ml). Neat ITZ produced a reduction of viability not higher than 10%. Neutral (uncoated) and cationic (DDAB coated) drug-loaded SLN reduced the cell viability, an effect that was more evident for the cationic systems. The addition

of ALA instead did not seem to affect cell viability. Neutral SLN showed modest cytotoxic activity against U937 cells, which was canceled by the addition of ALA. Conversely, the addition of ALA to unloaded cSLN and ITZ-cSLN, albeit with some improvement, failed to recover cell viability.

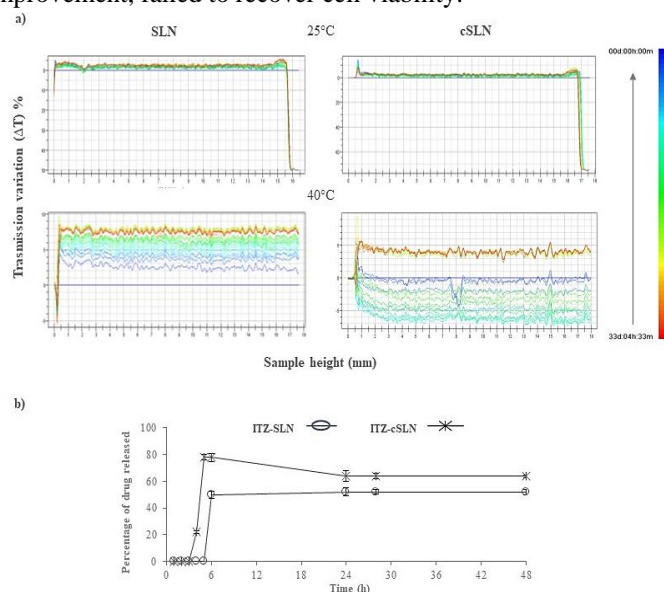


**Figure 1.** a) Turbiscan transmission profiles ( $\Delta T$ ) of unloaded SLN and cSLN stored at 25 °C and 40 °C. Data are shown as a function of time (0-33 days) of sample height (0 to 20 mm). The sense of analysis time is indicated by the arrow; b) In vitro release profile of ITZ from uncoated SLN and DDAB coated cSLN. Values are the average of almost three different experiments  $\pm$  standard deviation (SD).

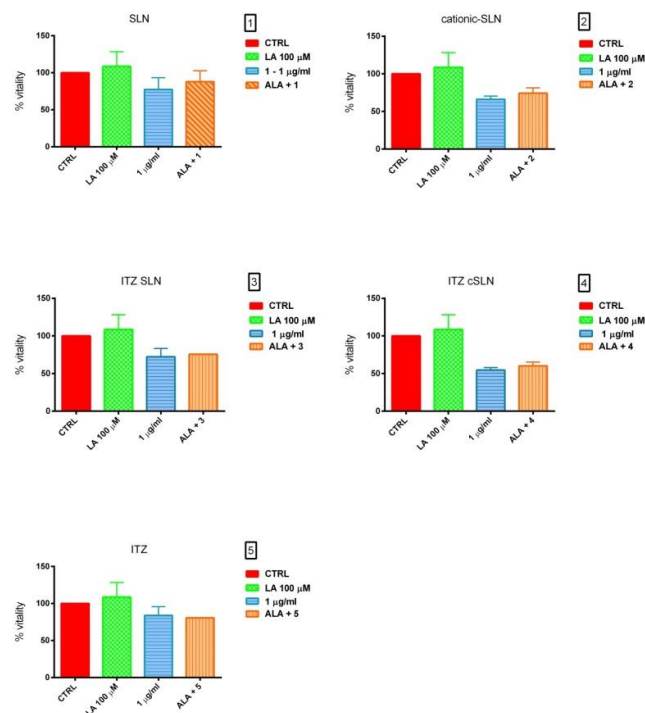


**Figure 2.** Cytotoxicity results on U937 cell line for: 1) neutral, unloaded SLN; 2) unloaded c-SLN; 3) ITZ-SLN; 4) ITZ-cSLN; 5) free ITZ.

#### 4. CONCLUSIONS

Loading SLN systems with antifungal agents can be a valid strategy to improve the efficacy of these drugs, enlarging their spectrum of action and reducing the effective dose. Furthermore,

positive changes in drug pharmacokinetics and stability could be achieved in successful cases. In this study, as a completion of a previous investigation on topical ITZ- SLN [7], this azole agent

was laden in uncoated (neutral) and DDAB-coated (cationic) SLN, obtaining very small and homogenous nanoparticle populations with the wished physico-chemical properties and a high drug entrapment efficacy. The SLN showed a very high physical stability over time and a sustained drug release profile.

Once loaded in the SLN, ITZ showed a reduction of MIC values against *Candida albicans*, compared to the neat drug. Cytotoxicity results on U937 tumor cell line demonstrated how a clear

correlation exists between the composition of the SLN matrix (and particularly their surface charge) and a decrease in cell viability. Given the relatively limited results, no other marker of cell toxicity was investigated.

The investigation on these carrier systems is continuing to deepen the mechanisms through which positively-coated and neutral SLN determine a certain degree of cytotoxicity, both when used alone or in association with ITZ.

## 5. REFERENCES

[1] Furneri P.M., Petronio G., Fuochi V., Cupri S., Pignatello R., Nanosized devices as antibiotics and antifungals delivery: past, news, and outlook, *Nanostructures for Drug Delivery*, Inc., E., Ed. 697-748, **2017**.

[2] Furneri P.M., Fuochi V., Pignatello R., Lipid-based Nanosized Delivery Systems for Fluoroquinolones: a Review, *Current Pharmaceutical Design*, **2017**.

[3] Gokce E.H., Ozyazici M., Souto E.B., Nanoparticulate strategies for effective delivery of poorly soluble therapeutics, *Therapeutic Delivery*, 1, 1, 149-67, **2010**.

[4] Pignatello R., Fuochi V., Petronio G., Greco A.S., Furneri P.M., Formulation and Characterization of Erythromycin-loaded Solid Lipid Nanoparticles, *Biointerface Research in Applied Chemistry*, 2145-2150, **2017**.

[5] Pignatello R., Leonardi A., Fuochi V., Petronio G., Greco A.S., Furneri P.M., A Method for Efficient Loading of Ciprofloxacin Hydrochloride in Cationic Solid Lipid Nanoparticles: Formulation and Microbiological Evaluation, *Nanomaterials*, 8, 5, **2018**.

[6] Mohanty B., Majumdar D.K., Mishra S.K., Panda A.K., Patnaik S., Development and characterization of itraconazole-loaded solid lipid nanoparticles for ocular delivery, *Pharmaceutical Development and Technology*, 20, 4, 458-64, **2015**.

[7] Carbone C., Martins-Gomes C., Pepe V., Silva A.M., Musumeci T., Puglisi G., Furneri P.M., Souto E.B., Repurposing itraconazole to the benefit of skin cancer treatment: A combined azole-DDAB nanoencapsulation strategy, *Colloids and Surfaces. B, Biointerfaces*, 167, 337-344, **2018**.

[8] Lestner J., Hope W.W., Itraconazole: an update on pharmacology and clinical use for treatment of invasive and allergic fungal infections, *Expert Opin Drug Met.*, 9, 7, 911-926, **2013**.

[9] Tsubamoto H., Inoue K., Sakata K., Ueda T., Takeyama R., Shibahara H., Sonoda T., Itraconazole Inhibits AKT/mTOR Signaling and Proliferation in Endometrial Cancer Cells, *Anticancer Research*, 37, 2, 515-519, **2017**.

[10] Keighley C.L., Manii P., Larsen S.R., van Hal S., Clinical effectiveness of itraconazole as antifungal prophylaxis in AML patients undergoing intensive chemotherapy in the modern era, *Eur J Clin Microbiol*, 36, 2, 213-217, **2017**.

[11] Saxena A., Becker D., Preeshagul I., Lee K., Katz E., Levy B., Therapeutic Effects of Repurposed Therapies in Non-Small Cell Lung Cancer: What Is Old Is New Again, *Oncologist*, 20, 8, 934-45, **2015**.

[12] Liang G., Liu M., Wang Q., Shen Y., Mei H., Li D., Liu W., Itraconazole exerts its anti-melanoma effect by suppressing Hedgehog,

Wnt, and PI3K/mTOR signaling pathways, *Oncotarget*, 8, 17, 28510-28525, **2017**.

[13] CLSI, M60 Performance Standards for Antifungal Susceptibility Testing of Yeasts. 1st ed., 2017. Clinical and Laboratory Standards Institute: Wayne, PA, USA, **2017**.

[14] Fuochi V., Volti G.L., Camiolo G., Tiralongo F., Giallongo C., Distefano A., Petronio G., Barbagallo I., Viola M., Furneri P.M., Di Rosa M., Avola R., Tibullo D., Antimicrobial and Anti-Proliferative Effects of Skin Mucus Derived from *Dasyatis pastinaca* (Linnaeus, 1758), *Marine Drugs*, 15, 11, **2017**.

[15] Carbone C., Cupri S., Leonardi A., Puglisi G., Pignatello R., Lipid-based nanocarriers for drug delivery and targeting: a patent survey of methods of production and characterization, *Pharmaceutical Patent Analyst*, 2, 5, 665-77, **2013**.

[16] Carbone C., Leonardi A., Cupri S., Puglisi G., Pignatello R., Pharmaceutical and biomedical applications of lipid-based nanocarriers, *Pharmaceutical Patent Analyst*, 3, 2, 199-215, **2014**.

[17] Carbone C., Campisi A., Manno D., Serra A., Spatuzza M., Musumeci T., Bonfanti R., Puglisi G., The critical role of didodecyldimethylammonium bromide on physico-chemical, technological and biological properties of NLC, *Colloids and Surfaces. B, Biointerfaces*, 121, 1-10, **2014**.

[18] Carbone C., Campisi A., Musumeci T., Raciti G., Bonfanti R., Puglisi G., FA-loaded lipid drug delivery systems: preparation, characterization and biological studies, *European Journal of Pharmaceutical Sciences*, 52, 12-20, **2014**.

[19] Carbone C., Manno D., Serra A., Musumeci T., Pepe V., Tisserand C., Puglisi G., Innovative hybrid vs polymeric nanocapsules: The influence of the cationic lipid coating on the "4S", *Colloids and Surfaces. B, Biointerfaces*, 141, 450-7, **2016**.

[20] Carbone C., Musumeci T., Lauro M.R., Puglisi G., Eco-friendly aqueous core surface-modified nanocapsules, *Colloids and Surfaces. B, Biointerfaces*, 125, 190-6, **2015**.

[21] Carbone C., Tomasello B., Ruozi B., Renis M., Puglisi G., Preparation and optimization of PIT solid lipid nanoparticles via statistical factorial design, *European Journal of Medicinal Chemistry*, 49, 110-7, **2012**.

[22] Teixeira M.C., Carbone C., Souto E.B., Beyond liposomes: Recent advances on lipid based nanostructures for poorly soluble/poorly permeable drug delivery, *Progress in Lipid Research*, 68, 1-11, **2017**.

[23] Carbone C., Arena E., Pepe V., Prezzavento O., Cacciatore I., Turkez H., Marrazzo A., Di Stefano A., Puglisi G., Nanoencapsulation strategies for the delivery of novel bifunctional antioxidant/signal selective ligands, *Colloids and Surfaces. B, Biointerfaces*, 155, 238-247, **2017**.

## 6. ACKNOWLEDGEMENTS

This work was supported by Research Funding for University of Catania, under Projects FIR 2014 and Piano per la Ricerca 2016-2018 - Linea di Intervento 2 "Dotazione Ordinaria" cod. 57722172106.

Authors declare no conflict of interest and that Ethical Approval was not required.

© 2018 by the authors. This article is an open access article distributed under the terms and conditions of the Creative Commons Attribution license (<http://creativecommons.org/licenses/by/4.0/>).